Journal of Computational Electronics 4: 63–66, 2005

Code for the 3D Simulation of Nanoscale Semiconductor Devices, Including Drift-Diffusion and Ballistic Transport in 1D and 2D Subbands, and 3D Tunneling

G. FIORI AND G. IANNACCONE
Dipartimento di Ingegneria dell'Informazione: Elettronica, Informatica, Telecomunicazioni, Università degli studi di Pisa, Via Caruso, I-56122, Pisa, Italy
g.fiori@iet.unipi.it

Abstract. We present a three-dimensional device simulator, suitable for the study of a wide range of nanoscale devices, in which quantum confinement and carrier transport are taken into account. In particular, depending on the confinement, the 1D, 2D or 3D Schrödinger equation with density functional theory in the local density approximation is coupled with the Poisson equation in the three-dimensional domain. Continuity equation in the ballistic and in the drift-diffusion regime are also solved assuming separation of the subbands.

Keywords: quantum modeling, ballistic transport, three-dimensional, Poisson

1. Introduction

Device modeling tools capable of addressing different degrees of quantum confinement and different transport regimes are required to study both MOSFETs at the end of the ITRS [1] Roadmap and device structures with alternative architectures. Commercial TCAD tools, in which current continuity and energy balance equations are implemented with quantum corrections, have provided useful insights of the present scaling approach, but for a complete understanding of the present and future device generations, a more accurate quantum approach is required. Indeed, even in MOSFETs of the latest technology node, quantum confinement of the electrons in the channel is significant, and energy levels split in well-separated 2D subbands [2,3]. Quantum models are then necessary to extract all the relevant electrical quantities also far from equilibrium, considering important phenomena that can occur at such dimensions like ballistic or quasi-ballistic transport [4]. In addition, while conventional planar MOSFETs are nowadays the most common devices, in the medium-long term they are going to be substituted by more promising architectures that offer better scalability perspectives for 10 nm channel lengths and beyond, such as multiple-gate SOI transistors [5,6]. In such devices, transport occurs through one-dimensional subbands [7], since carriers are confined in the two-dimensional plane perpendicular to the current direction and quantum tunneling may be significant [8]. A versatile device simulator must also be capable of considering at the same time different kinds of confinements as is the case in nanocrystal memories [9] or in Single Electron Transistors [10]. In this work, we present the *ViDES* (Versatile DEvice Simulator) code, based on the self-consistent solution in 3D of the (i) many particle Schrödinger equation based on density functional theory in the effective mass approximation, (ii) nonlinear Poisson equation, and (iii) continuity equation for electrons, in the cases of both drift-diffusion and ballistic transport regimes. In addition, regions with different degrees of quantum confinement may be considered, and transport in such regions is consequently computed. If in a given region charge carriers are quantum confined in two directions (1D confinement), transport (ballistic or drift-diffusive) is computed in 1D subbands. Analogously, if charge carriers are confined in one direction (2D confinement), transport is computed in 2D subbands.

2. Code Architecture and Models

The core of the device simulator is represented by the three-dimensional Poisson solver, which is discretized over a rectangular grid and it is based on the Newton-Raphson algorithm with the predictor/corrector scheme proposed in [11].

Independent modules, in which quantum models with different degrees of confinement are implemented, provide the electron concentration n and its derivative with respect to the electrostatic potential ϕ to the Poisson solver, which, in turns, gives back in a self-consistent iteration scheme ϕ needed to compute n itself (Fig. 1).

In all the modules the Schrödinger equation is solved in strongly confined regions in the effective mass approximation with the Density Functional Theory, Local Density Approximation, while a semiclassical approximation (using either the Fermi-Dirac or Maxwell-Boltzmann distributions) is assumed elsewhere.

In addition, ellipsoidal parabolic energy bands are taken into account, hence the Schrödinger equation is solved for each effective mass along the k-space directions.

In this way, as pointed out in the previous section, different kinds of confinement can be considered at the same time in different regions of the same device. In particular, if quantum confinement is predominant along one direction, the one-dimensional Schrödiger equation is solved in the direction of strong confinement and a semiclassical expression for in-plane states is assumed [12], while, if the confinement is predominant in two-dimensions, the two-dimensional Schrödinger equation is solved in the plane of confinement, and continuous states are considered in the direction of propagation [13].

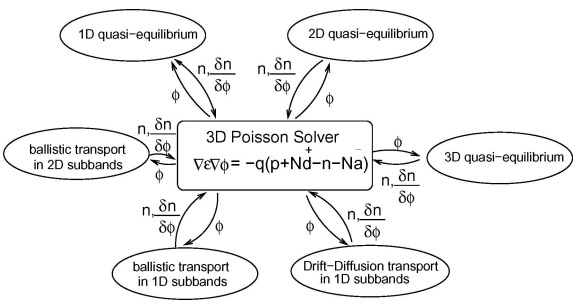

Figure 1. Sketch of the code architecture.

A different approach has been followed in the module that compute the 3D confined quantum electron density. In particular, we have fixed the number of electrons in the confined region, so that the electron density can be expressed as

$$n_{3D} = 2\sum_{i=1}^{m} |\psi_i|^2 + (N - 2m)|\psi_{m+1}|^2 , \qquad (1)$$

where ψ_i is the orbital associated to the i-th eigenvalue, N is the total number of electrons in the dot, and $m = \lfloor \frac{N}{2} \rfloor$ is the number of fully occupied single electron levels.

This choice has been dictated by the need to determine the electrochemical potential of a three-dimensional confined region, that can be easily computed by means of the Slater formula [14]. Indeed, the electrochemical potential $\mu(N)$, defined as the energy necessary to add the N-th electron to the dot, can be expressed as

$$\mu(N) = E(N) - E(N-1) = \varepsilon\left(N - \frac{1}{2}\right), \qquad (2)$$

where E is the total energy of the dot, while ε is the energy of the half-occupied highest Kohn-Sham orbital of a system with $N - \frac{1}{2}$ electrons. Due to its modularized structure, the code is a very versatile tool since allows the developer to easily include different models in the program framework. This is valid not only for models at the quasi-equilibrium as those discussed above, but also for models far from the equilibrium. Indeed, our code also includes modules in which transport through well separated subbands is computed. In particular, the continuity equation in both the ballistic and in the drift-diffusion approximation is solved in 1D subbands, as well as ballistic transport in 2D subbands.

When transport between two regions occurs via tunneling, the two regions are typically considered electrically insulated, so that the continuity equation is not solved in the self-consistent scheme. Then, once the potential and charge profiles are obtained, as a post processing procedure tunneling currents are computed using a routine for the computation of scattering matrices in three-dimensional domains.

3. Simulations

In this section we present a wide range of examples, showing that our code can be used to address a broad variety of nanoscale devices.

3.1. *Single Electron Transistor*

First, we present an example of the simulation of a single electron transistor defined by split gates on an AlGaAs/GaAs heterostructure. In Fig. 2(a) the gate layout of the considered device is depicted, while in Fig. 2(b) the equivalent capacitance circuit is shown. Two different types of confinement have been taken into account in the same domain: three-dimensional in the central region corresponding to the dot, and one-dimensional in the two-dimensional electron gas (2DEG). The electrochemical potential, computed with Slater's rule, is shown in Fig. 3 as a function of the gate voltage applied to gates 2 and 5, and it can be used to extract the capacitances of the equivalent circuit. The drain-to-source conductance as a function of the gate voltage can be easily obtained from the computation of the conductance of each quantum constriction in correspondence of the gate voltage for which the electrochemical potential aligns with the Fermi level.

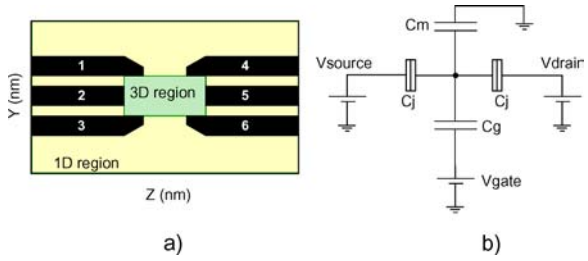

Figure 2. (a) Split gate layout and considered quantum confinement; (b) Equivalent capacitance circuit.

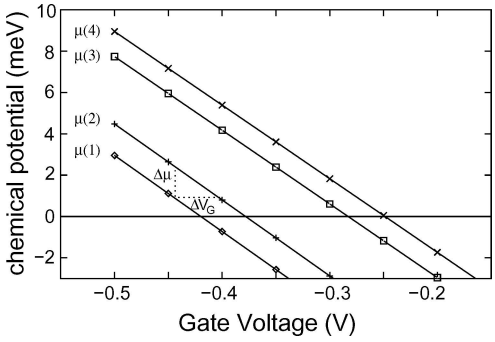

Figure 3. Computed electrochemical potential as a function of the voltage applied to gates 2 and 5.

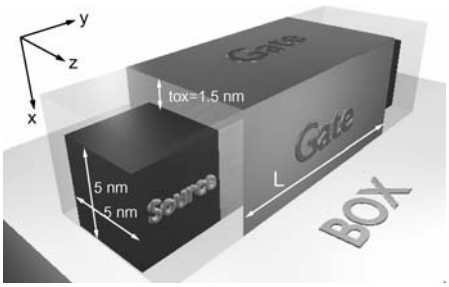

Figure 4. Structure of the considered SNWT.

3.2. *Silicon Nanowire Transistor*

As a second example, we present the simulation of a silicon nanowire transistor (SNWT), whose structure is shown in Fig. 4, with channel length $L = 7$ nm and channel cross-section of 5×5 nm^2. Here, quantum confinement occurs in the x and z directions while transport in one-dimensional subbands in the y direction. For such geometries, 1D subbands are well separated, so transport can be studied independently in each subband. We have considered a fully ballistic transport in the channel, both in the semiclassical and in the quantum case (i.e. considering barrier tunneling), and, in addition, we have solved the drift/diffusion equation in each 1D subband taking into account velocity saturation: in this way we have been able to define an upper (fully ballistic transport) and a lower limit (drift/diffusion transport) for the device performance, as well as to study the influence of quantum transport on device characteristics. In Fig. 5 we plot the transfer

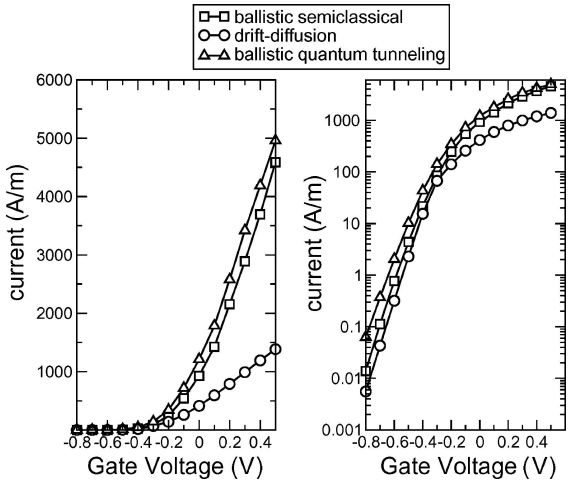

Figure 5. Transfer characteristics of the SNWT device with channel length equal to 7 nm in the linear and in the logarithmic scale.

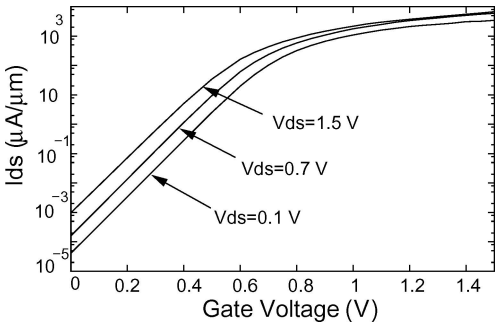

Figure 6. Transfer characteristic computed in the ballistic approximation for a 25 nm Well-Tempered MOSFET.

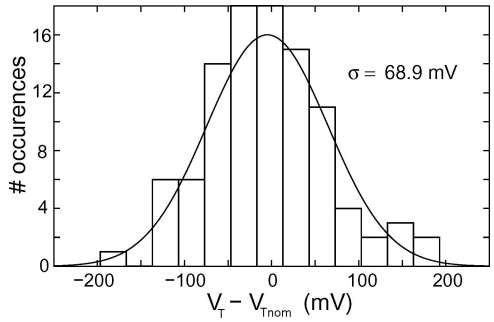

Figure 7. Threshold voltage shift dispersion computed over a sample of 100 devices. V_{Tnom} is the threshold voltage computed in case of uniform doping profile.

characteristics obtained by assuming Drift-diffusion transport in the 1D subbands, and ballistic transport, both including or not including source-to-drain tunneling.

3.3. Well-Tempered MOSFETs

As a last example, we show results for a Well-Tempered MOSFET with 25 nm channel length [15]. Confinement is predominant along the direction perpendicular to the Si/SiO_2 interface, and splitting of the energy level in two-dimensional subbands occurs. Ballistic transport has been computed over the well-separated subbands and transfer characteristic are shown in Fig. 6.

For such devices, other effects such as the random distribution of dopants in the depletion region plays an important role. Simulating a large number of devices with the same nominal doping profile, but with a different actual one, we have also computed the standard deviation of the threshold voltage extracted from the transfer characteristics computed in the drift-diffusion approximation, as shown in Fig. 7.

4. Conclusions

In conclusion, we have presented a three-dimensional Poisson/Schrödinger solver which results to be a very versatile tool for the investigation of the electrical properties of a broad range of nanoscale semiconductor devices, both at the quasi-equilibrium and far from the equilibrium. We have shown that our code is able to consider different kinds of confinement as well as different transport mechanism, that allow us to extract all the relevant electrical quantities.

We gratefully acknowledge support from the EU through the project NANOTCAD and the Network of Excellence SINANO, and from the Fondazione Cassa di Risparmio di Pisa.

References

1. International Technology Roadmap for Semiconductors 2003, Semiconductor Industry Association, S. Josè, USA (http://public.itrs.net).
2. Y. Taur and T.H. Ning, *Fundamentals of Modern VLSI devices* (Cambridge University Press, Cambridge UK, 1998), p. 194.
3. Y. Taur, D.A. Buchanan, W. Chen, D.J. Frank, K.E. Ismail, S.H. Lo, G.A. Sail-Lalasz, R.G. Viswanathan, H.J.C. Wann, S.J. Wind, and H.S. Wong, *Proc. IEEE*, **85**, 486 (1997).
4. Z. Ren, R. Venugopal, S. Datta, and M. Lundstrom, *IEDM tech. Dig.*, 715 (2000).
5. E. Suzuki, K. Ishii, S. Kanemaru, T. Maeda, T. Tsutsumi, T. Sekigawa, K. Nagai, and H. Hiroshima, *IEEE Trans. Electron Devices*, **47**, 354 (2000).
6. J.P. Colinge, J.T. Park, and C.A. Colinge, *MIEL 2002, Proceedings*, 109 (2002).
7. J. Wang, E. Polizzi, and M. Lundstrom, *IEDM Tech. Dig.*, 29 (2003).
8. T.J. Walls, V.A. Sverdlov, and K.K. Likharev, *Solid-State Electron.*, **48**, 857 (2004).
9. G. Iannaccone and P. Coli., *Appl. Phys. Lett.*, **78**, 2046, (2001).
10. A. Scholze, A. Schenk, and W. Fichtner, *IEEE Trans. Electron Devices*, **47**, 1811 (2000).
11. A. Trellakis, A.T. Galick, A. Pacelli, and U. Ravaioli, *J. Appl. Phys*, **81**, 7800 (1997).
12. G. Fiori and G. Iannaccone, *Nanotechnology*, **13**, 294 (2002).
13. S. Datta, *Electronic Transport in Mesoscopic Systems* (Cambridge University Press, Cambridge UK, 1998), p. 29.
14. J.C. Slater, *Phys. Rev.*, **81**, 385 (1951).
15. www-mtl.mit.edu/Well